ELSEVIER

PII: S0032-3861(96)00906-8

Polymer Vol. 38 No. 14, pp. 3513–3520, 1997

0032-3861/97/$17.00+0.00

Blends of homogeneous ethylene–octene copolymers

S. Bensason, S. Nazarenko, S. Chum*, A. Hiltner† and E. Baer
Department of Macromolecular Science and Center for Applied Polymer Research, Case Western Reserve University, Cleveland, OH 44106, USA
**Polyolefins and Elastomers Research and Development, The Dow Chemical Company, Freeport, TX 77541, USA*
(Received 11 June 1996; revised 28 August 1996)

Blends of ethylene–octene copolymers prepared by Dow's INSITE™ constrained geometry catalyst and process technology were characterized. (INSITE™ is a trademark of The Dow Chemical Company.) A previously described classification scheme based on density, or comonomer content, was the basis for the choice of blend components. The blends combined a low density Type I copolymer (0.865 g cm^{-2}) with a higher density copolymer. The second component was either another Type I copolymer (0.887 g cm^{-3}), a Type II copolymer (0.901 g cm^{-3}), or a Type III copolymer (0.913 g cm^{-3}). The melting and crystallization behaviour suggested that the components crystallized separately in all the blends. However, dynamic mechanical analysis indicated that the noncrystalline portions of the Type I blends formed a single phase, whereas the noncrystalline regions of blends with the Type II or Type III copolymer appeared to be phase separated in the solid state. The stress–strain behaviour at ambient temperature correlated with density, or total crystallinity, regardless of whether the material was a copolymer or a blend. © 1997 Elsevier Science Ltd.

(Keywords: polyethylene blends; ethylene–octene copolymers)

INTRODUCTION

Copolymers of ethylene and α-olefins produced by conventional multisite catalysts, generally referred to as linear low density polyethylenes or LLDPEs, are complex mixtures by composition and molecular weight[1,2]. There is evidence that the chain-to-chain heterogeneity of a typical LLDPE is broad enough to produce thermodynamically driven microphase separation in the melt[3]. Although the implications of phase heterogeneity in LLDPE with regard to properties are not well understood, there is speculation that discrete domains of rubber-like material produced by phase segregation of highly branched non-crystallizable molecules contribute to the unusually high toughness of many LLDPEs[4,5].

Cocrystallization in heterogeneous mixtures of polyethylene molecules is also an important aspect of the phase structure. Studies of blends reconstituted from LLDPE fractions have provided insight into crystallization and solid state morphology, and specifically have demonstrated that LLDPE incorporates fractions that do not cocrystallize[6]. The desire to achieve an optimum balance of physical properties, toughness and processability has motivated studies of cocrystallization in LLDPE blends with HDPE and LDPE[7–11]. Although blending LLDPE with other polyethylenes can give interesting information on morphology and property effects, the composition of these blends is even more complex than that of LLDPE alone. Recent studies utilized homogeneous copolymers[12] or hydrogenated polybutadiene copolymers[13–15] to probe the phase structure of blends. Although most of these studies did not extend to structure–property relationships, there is a suggestion that the ultimate properties are enhanced by cocrystallization[16].

The recent development of Dow's INSITE™ constrained geometry catalyst and process technology has made available copolymers of ethylene with α-olefins that differ significantly from conventional LLDPEs in having narrow molecular weight distribution, homogeneous comonomer distribution and homogeneous long chain branching structure. Furthermore, it is possible to polymerize copolymers with lower densities and crystallinities than the conventional LLDPEs[17,18]. As the comonomer content increases, the accompanying tensile behaviour changes from necking and cold drawing typical of a semicrystalline thermoplastic to uniform drawing and high recovery characteristic of an elastomer. Although solid state structure and properties change gradually with increasing comonomer content, the large contrast between the extremes in comonomer content suggested a classification scheme based on density or comonomer content[19]. The combined body of observations from melting behaviour, morphology, dynamic mechanical response, yielding, and large-scale deformation led to classification of INSITE™ copolymers into four distinct types. Materials with densities higher than 0.93 g cm^{-3}, Type IV, exhibit a lamellar morphology with well-developed spherulitic superstructure. Type III polymers with densities between 0.93 and 0.91 g cm^{-3} have thinner lamellae and smaller spherulites. Type II materials with densities between 0.91 and

† To whom correspondence should be addressed

Table 1 INSITE™ ethylene–octene copolymers

Polymer designation	Comonomer content[a] (mol%)	Density ($g\,cm^{-3}$)	I_2 ($g\,10\,min^{-1}$)	I_{10}/I_2
Type I base	14.6	0.865	0.5	≈8.5
Type I	8.5	0.887	1.0	9.2
Type II	5.3	0.901	1.0	9.0
Type III	3.3	0.913	1.0	10.5

[a] Calculated from density[17]

Table 2 Composition and density of INSITE™ blends

Blends (v/v)	Blending ratio (w/w)	Density ($g\,cm^{-3}$)	Calculated density ($g\,cm^{-3}$)
	IB-I Blends		
75/25	74.6/25.4	0.871	0.870
50/50	49.4/50.6	0.877	0.876
25/75	24.6/75.4	0.882	0.881
	IB-II Blends		
75/25	74.3/25.7	0.875	0.874
50/50	49.0/51.0	0.884	0.883
25/75	24.3/75.7	0.893	0.892
	IB-III Blends		
75/25	74.0/26.0	0.888	0.877
50/50	48.7/51.3	0.890	0.889
25/75	24.1/75.9	0.901	0.901

$0.89\,g\,cm^{-3}$ have a mixed morphology of small lamellae and fringed micellar crystals, and can form very small spherulites. Type I copolymers with densities less than $0.89\,g\,cm^{-3}$ have no lamellae or spherulites; fringed micellar crystals are inferred from the low degree of crystallinity, the low melting temperature, and the granular, nonlamellar morphology.

The availability of homogeneous ethylene copolymers presents an opportunity to probe the limits imposed by branch concentration, branch length and molecular weight on miscibility of ethylene copolymer blends. Insight into the phase structure of the melt, and the crystalline and noncrystalline regions of the resulting solid state, can subsequently be used to tailor blend composition for controlled phase morphology and optimized properties. This initial study of INSITE™ blends focuses on binary blends that combine an INSITE™ copolymer having a high branch concentration with a series of other INSITE™ copolymers of approximately the same molecular weight but of progressively decreasing branch concentration. The choice of components is based on the previous classification of INSITE™ copolymers[19]. Thus a low density copolymer with fringed micellar crystals (Type I) is combined with another Type I copolymer, or with a slightly higher density copolymer with a mixed morphology of fringed micelles and small lamellae (Type II), or with a higher density copolymer with lamellar morphology (Type III). The blends were characterized by differential scanning calorimetry, dynamic mechanical analysis, and tensile stress–strain behaviour. Although these classical techniques are often inconclusive for blends of conventional ethylene copolymers, they may be more revealing for blends of the compositionally homogeneous INSITE™ copolymers.

MATERIALS AND METHODS

Materials

Four ethylene–octene copolymers synthesized by the Dow INSITE™ technology were used in the study. The resins had approximately the same molecular weight, the principal microstructural variable was the comonomer content. The comonomer content (mol%), the melt flow index (I_2), and the ratio of melt flow indices at loads of 10 and 2.16 kg (I_{10}/I_2) as given in *Table 1* were provided by The Dow Chemical Company, Freeport, TX. Binary blends with compositions 25/75, 50/50 and 75/25 (vol/vol) were prepared from the resin with the lowest density (Type IB) and three resins with higher densities (Type I,

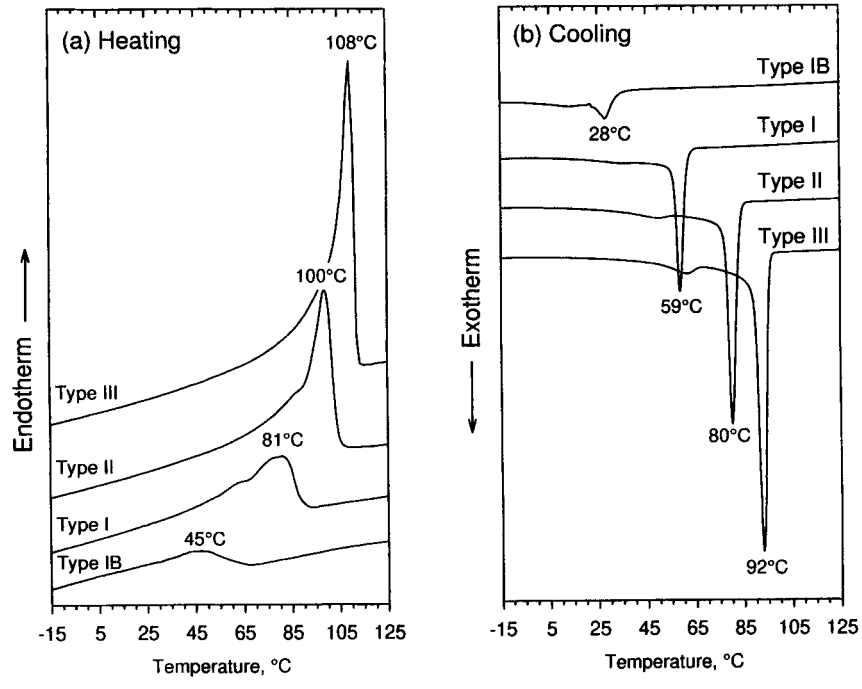

Figure 1 Thermograms of component polymers: (a) second heating scans; and (b) cooling scans

Type II and Type III). The resin densities in *Table 1* were used to determine the required blend compositions (wt/wt). The compositions of the blends and the resulting densities are given in *Table 2*.

Methods

Melt blending was carried out in a Haake Rheomix 600 mixing head with 40 cm^3 mixing volume. Copolymer blends were processed at 160°C for 8 min at 50 rpm under dry nitrogen. Single copolymers were processed under identical conditions to give them the same thermal history as the blends. The temperature of the melt rose about 10°C to 170°C during mixing. After cooling, the polymer was compression moulded into 1.4 mm thick plaques. The material was sandwiched between Mylar sheets, heated at 190°C for 2 min under minimal pressure, then for 5 min at 275 psi and 1 min at 800 psi. The plaques were rapidly cooled by plunging into ice water.

Densities of the quenched plaques were measured within 24 h of moulding in an isopropanol-distilled water density gradient column calibrated with glass floats. The average of three measurements is reported in *Tables 1* and *2*. The accuracy was $\pm 0.0002\ g\,cm^{-3}$. The measured densities of the blends agreed with values calculated by assuming additivity of the components, *Table 2*.

Thermal analysis was carried out in a Perkin–Elmer Model 7 DSC with approximately 5 mg specimens cut from the plaques. The thermograms were obtained with a heating/cooling rate of $10°C\,min^{-1}$ unless otherwise indicated. First heating thermograms were obtained from −50° to 190°C. The specimens were held at 190°C for 10 min before cooling to −50°C and then subjected to a second heating cycle with identical conditions as the first. Crystallinity calculations were based on a heat of fusion of $290\ J\,g^{-1}$ for the polyethylene crystal.

Dynamic mechanical measurements were carried out in a DMTA MkII unit from Polymer Laboratories (Amherst, MA) operating in the single cantilever mode. The specimen thickness and width were approximately 1.4 mm and 5 mm, and the length was 5 mm. Measurements were taken at a frequency of 1 Hz, the temperature was raised from −150°C to the melting point at a heating rate of $2°C\,min^{-1}$.

Stress–strain behaviour in uniaxial tension was determined on ASTM 1708 microtensile specimens cut from the compression moulded plaques. The specimens were stretched in an Instron 1123 universal testing machine at a rate of $10\,min^{-1}$.

RESULTS AND DISCUSSION

Melting and crystallization

The melting behaviour of the four copolymers used in the blends is illustrated with second heating thermograms in *Figure 1a*. The first heating always exhibited an additional peak at about 38°C; this was attributed to melting of crystals that formed while the material aged at ambient temperature[18]. All copolymers showed broad melting endotherms with a long low temperature tail. The melting peak shifted to a lower temperature, from 108 to 100 to 81 to 45°C, and the melting enthalpy decreased with increasing comonomer content. An

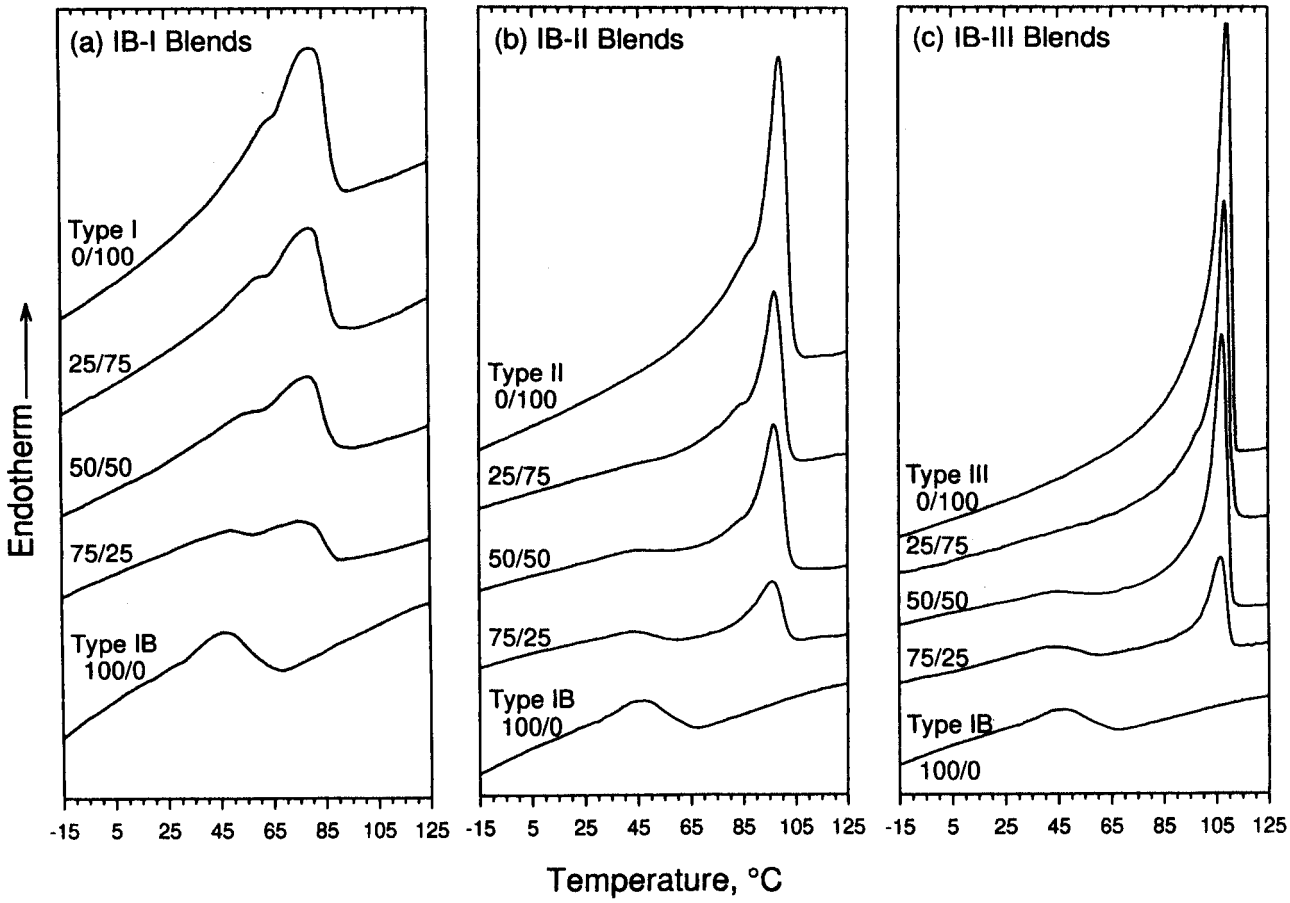

Figure 2 Heating thermograms of blends: (a) Type IB-I blends; (b) Type IB-II blends; and (c) Type IB-III blends

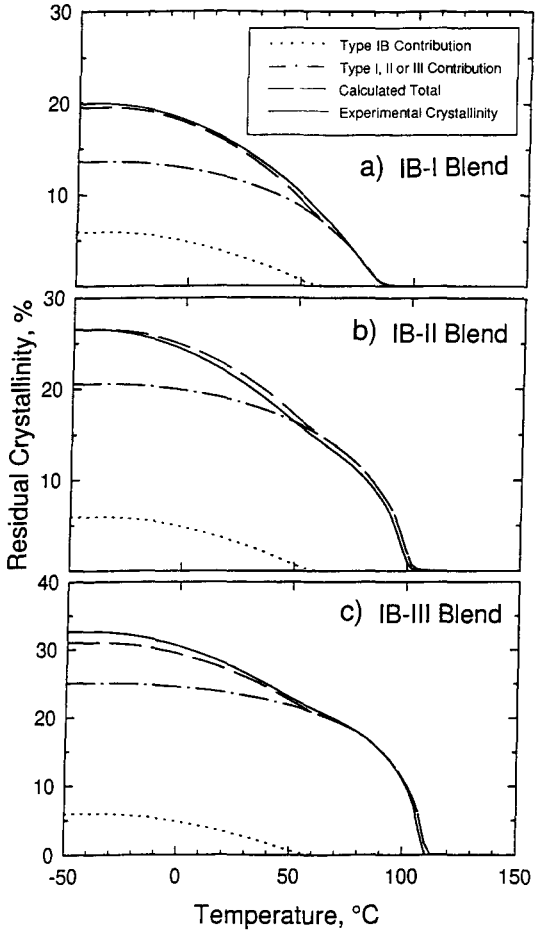

Figure 3 Comparison of the residual crystallinity in 50/50 blends with that calculated from the contributions of the individual components: (a) the Type IB-I blend; (b) the Type IB-II blend; and (c) the Type IB-III blend

additional small peak or shoulder was observed slightly below the primary melting peak in both first and second heating thermograms of the Type II and Type III materials.

Cooling thermograms of the copolymers all showed a large crystallization peak followed by a small exotherm about 35°C lower in temperature, *Figure 1b*. Increased branching resulted in a decrease of the crystallization temperature and the crystallization enthalpy. The small additional peaks in both the heating and cooling thermograms are often observed in ethylene copolymers and their blends, and several explanations have been proposed[20].

Melting thermograms of Type IB-I, IB-II and IB-III blends are compared in *Figures 2a–c*. Second heatings were used for comparison in order to avoid the effects of ambient temperature annealing. All the 50/50 and 75/25 blends exhibited two distinct melting peaks that corresponded to those of the components. Only the melting peak of the less branched component was observed in the 25/75 blends. This was not unexpected because of the low crystallinity of the Type IB copolymer. The absence of any shift in the melting temperatures indicated that the two components crystallized as separate crystal populations in all the blends. Faster cooling from the melt might have facilitated cocrystallization in the blends. However the first heating thermograms of specimens taken from the quenched plaques revealed the same melting behaviour as the second heating thermograms; moreover, the same thermograms were obtained after quenching at a rapid cooling rate (200°C min^{-1}) in the d.s.c.

The concept of two separate crystal populations in the blends was examined by testing the additivity of crystallinity over the melting range. The residual crystallinity as a function of temperature was obtained by integrating the first heating thermograms. The residual crystallinities of the component copolymers were added proportionally to obtain the residual crystallinity of the blend. The plots in *Figures 3a–c* include the proportional contribution of each component to the 50/50 blend, the calculated crystallinity which is the sum of the two contributions, and the experimental crystallinity obtained by integrating the heating thermogram of the blend. Excellent agreement between the calculated curves and the experimental results supports the conclusion that the component copolymers form separate crystalline phases in all the blends.

Crystallization behaviour of the two components can provide evidence of the phase morphology in the melt[21–23]. The melt morphology is not of specific concern here, and definitive conclusions are not expected. Nevertheless, it will be instructive to compare possible melt morphologies with the phase state of the amorphous regions as interpreted from d.m.t.a. of the resulting solid state. In a homogeneous melt, crystallization kinetics of the components would be expected to depend on blend composition; alternatively, in a biphasic melt the kinetics would not be strongly affected. The crystallization behaviour of Type IB-I, IB-II and IB-III blends is compared in the cooling thermograms in *Figure 4*. All thermograms of the blends exhibited two crystallization peaks. For the 25/75 and 50/50 Type IB-II and Type IB-III blends, the endothermic peak temperatures corresponded to the crystallization temperatures of the components. For 75/25 blends, a 10°C decrease in crystallization temperature of the less branched component was observed. This is consistent with crystallization in Type IB-III and Type IB-II blends from a biphasic melt. The shift in crystallization temperature in blends with a small amount of the Type III or Type II component may be due to smaller domains in the biphasic melt that amplify interfacial effects; alternatively, slight miscibility of Type II and Type III with Type I in the melt could affect nucleation in blend compositions with small amounts of the higher melting component.

In contrast, the crystallization peak of the less branched component in the Type IB-I blends decreased continuously with increasing amount of Type IB in the blend, *Figure 5*. The continuous shift in the crystallization peak temperature suggested that Type I copolymers may be miscible in the melt, in which case nucleation kinetics of the less branched material would be affected at all blend compositions. This is in contrast to blends of Type IB with Type II and Type III copolymers where both melting behaviour and crystallization behaviour were consistent with a biphasic melt.

The noncrystalline regions constitute a larger portion of the solid state than the crystalline regions. The phase state of these regions was probed by dynamic mechanical analysis. The loss tangent and loss modulus for the blends and the component copolymers are shown in *Figures 6a–c*. For low crystallinity copolymers, Type IB and Type I, the β relaxation at about −40°C has the effect of a glass transition insofar as it is characterized by an intense peak

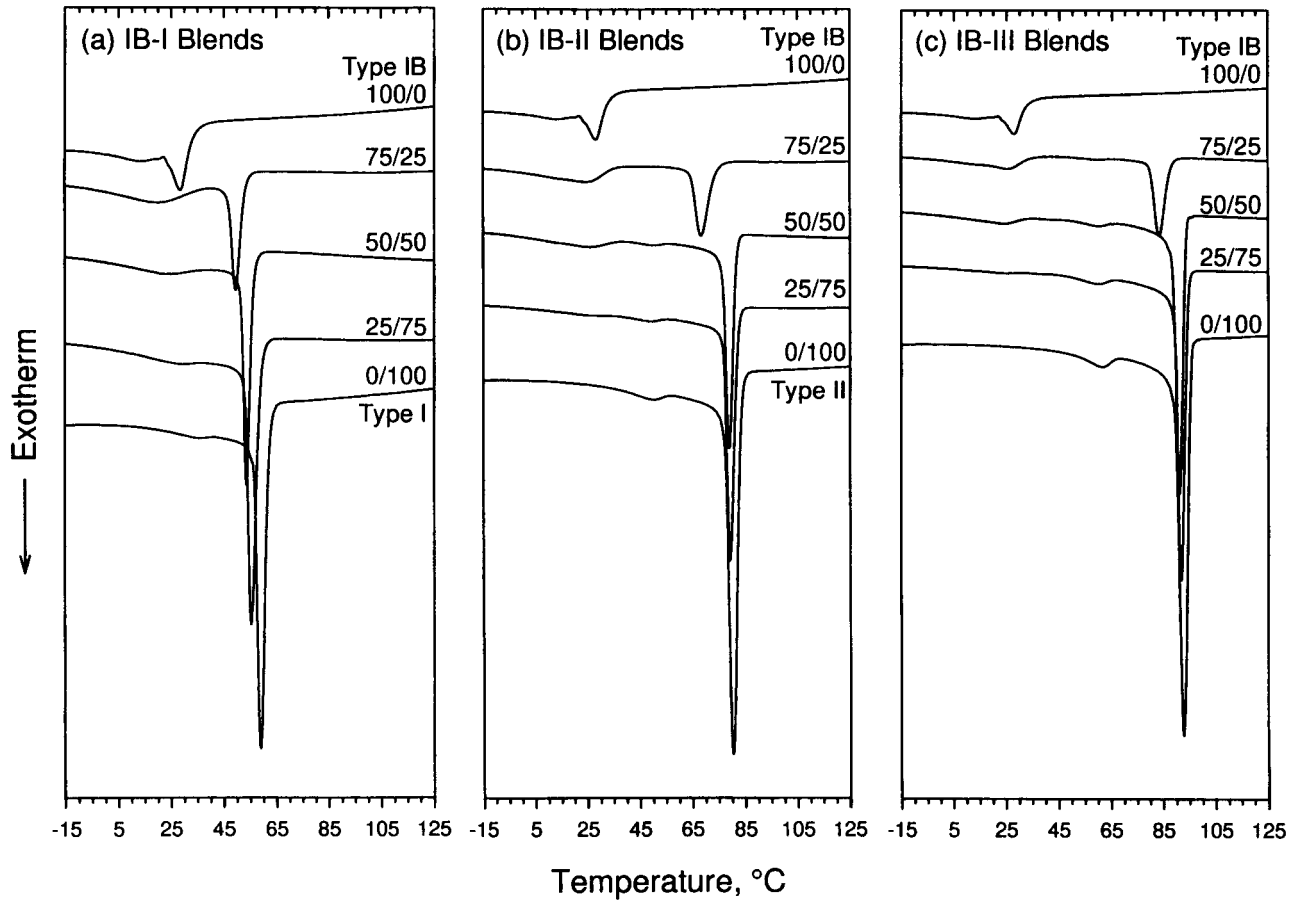

Figure 4 Cooling thermograms of blends: (a) Type IB-I blends; (b) Type IB-II blends; and (c) Type IB-III blends

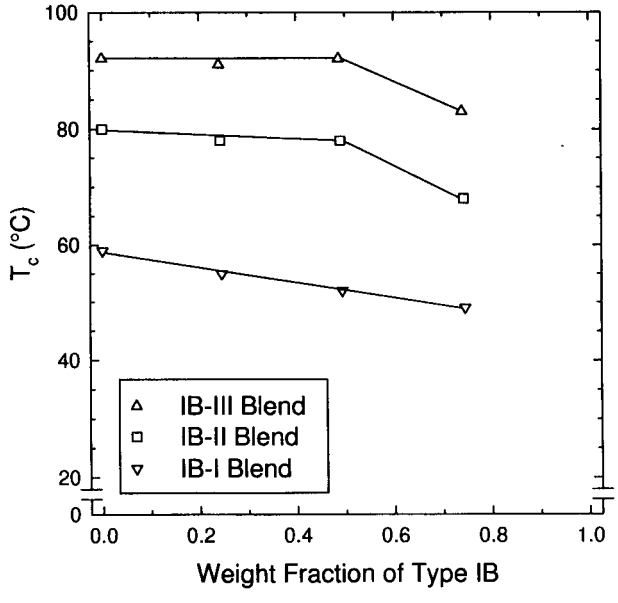

Figure 5 Crystallization temperature as a function of blend composition

in tan δ and is accompanied by a large drop in modulus. The Type IB-I blends all exhibited a single β relaxation at a temperature intermediate between those of the component copolymers. With increasing amount of Type I in the blend, the transition temperature gradually increased and the intensity gradually decreased as the peak approached that of the Type I component. This result suggests that the noncrystalline portions of Type IB and Type I form a single phase in the solid state. This pair of copolymers may be similar enough in composition that they are miscible in the melt, and that the noncrystalline components remain miscible after crystallization.

In copolymers of higher crystallinity, Type II and Type III, the β transition is reduced in intensity and the α transition becomes more prominent. All the Type IB-II and Type IB-III blends exhibited two relaxation peaks that could be resolved as the β relaxation of the Type IB component and the broader α–β relaxation of the higher crystallinity component. The exception was the Type IB-II 25/75 blend where the peaks overlapped and could not be resolved. There were no significant shifts in the relaxation temperatures of the components in the blends, especially for the Type IB-III blends. Thus, it appears that the noncrystalline portions of these copolymers are also immiscible. This would extend indications regarding the biphasic melt of Type IB-II and Type IB-III blends to the solid state.

Stress–strain relationship

Blends of Type IB and Type I combined components that are the most similar in terms of their stress–strain behaviour. Typically, deformation of Type I copolymers is macroscopically uniform and the stress–strain curve reveals elastomeric behaviour with a low initial modulus and at higher strains a gradually increasing slope[19]. Stress–strain curves of the Type IB and Type I components in *Figure 7a* showed that decreasing branch concentration increased the stress level at all strains and decreased the ultimate fracture strain. Curves for the Type IB-I blends, also included in *Figure 7a*, were

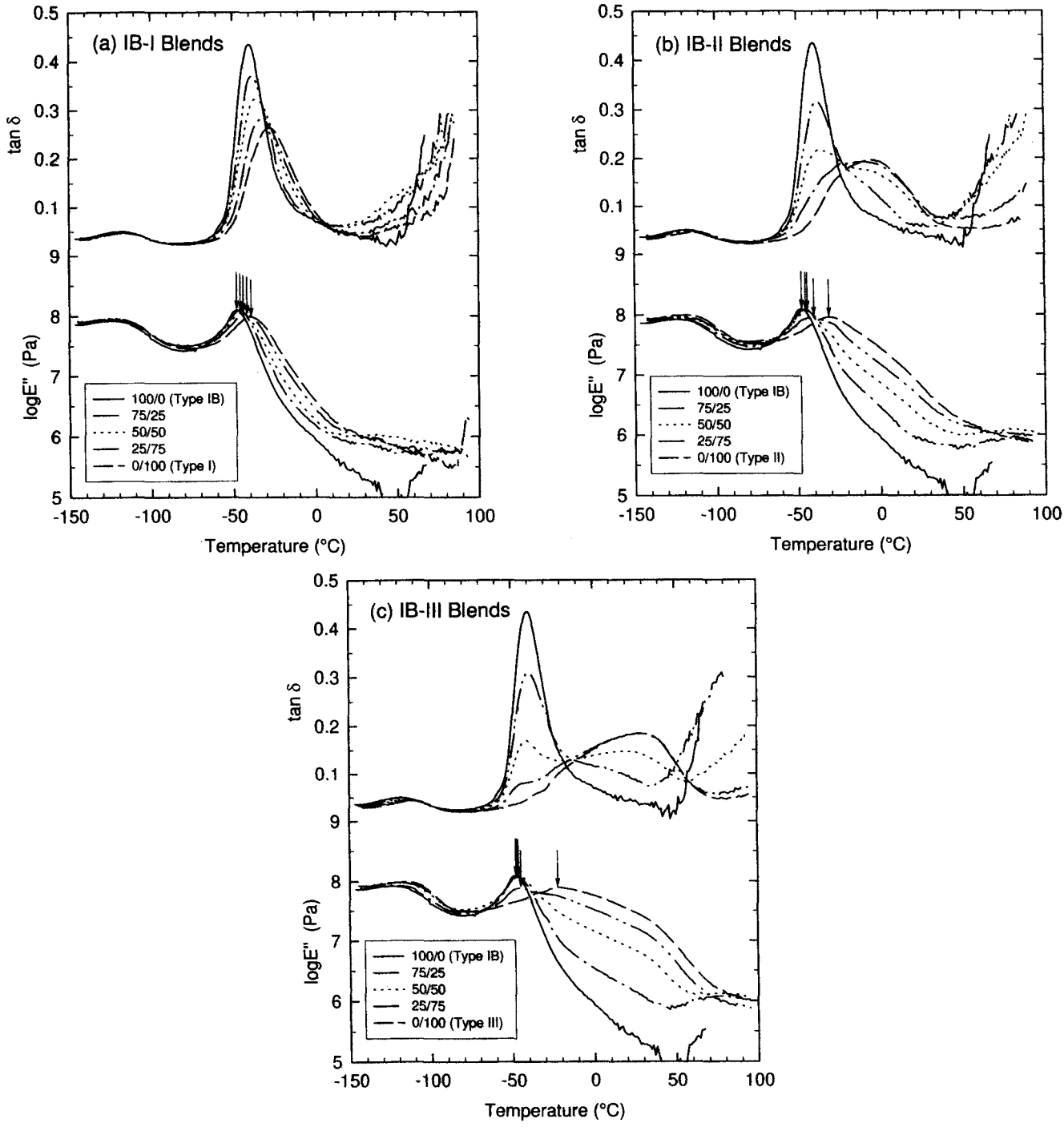

Figure 6 Dynamic mechanical spectra (tan δ and E'') of blends: (a) Type IB-I blends; (b) Type IB-II blends; and (c) Type IB-III blends

intermediate between those of the components. Thus, the stress at all strains gradually increased and the fracture strain gradually decreased as the amount of Type IB in the blend was raised. For comparison, calculated stress–strain curves for the blends were obtained from the stress–strain curves of the component copolymers by assuming additivity. As shown by the dashed lines in *Figure 7a*, these coincided very closely to the measured curves.

Stress–strain curves for Type IB-II and Type IB-III blends are shown in *Figures 7b and c*. Blends of Type IB and Type III combined copolymers that differed the most in terms of their stress–strain behaviour. In contrast to the elastomeric behaviour of Type IB, the Type III copolymer exhibited a yield maximum in the stress–strain curve that coincided with formation of a shallow neck. A short region of cold drawing followed. The blends exhibited intermediate behaviour with a gradual transition from Type III to Type IB behaviour, *Figure 7c*. The blend with the highest fraction of Type III, the (25/75) blend with density of 0.901 g cm^{-3}, did not exhibit a yield maximum although yielding was inferred from the changes in slope where the yield point was expected. Nonuniform deformation was confirmed by carefully measuring the draw ratio on the specimen. Blends with larger fractions of Type IB deformed uniformly with stress levels intermediate between Type III and Type IB copolymers. Calculated stress–strain curves assuming additivity of the component copolymers approximately reproduced the stress–strain curves of the

blends although the comparison was not as good as with the Type IB-I blends.

It was possible to compare the stress–strain behaviour of two copolymers with blends having similar densities, *Figure 8*. The densities of the Type I copolymer and the Type IB-II (50/50) blend were similar (0.88 g cm^{-3}), and likewise the densities of the Type II copolymer and the Type IB-III (25/75) blend (0.90 g cm^{-3}). The stress–strain curves corresponded closely up to moderate strains of about 400%. The similarity of the 0.90 g cm^{-3} materials included the characteristic slope changes in the yield region. It appears that stress–strain behaviour at ambient temperature correlates with density, or total crystallinity, regardless of whether the material is a INSITE™ copolymer or a blend of two INSITE™ copolymers. The blends necessarily have a broader range of bundled and lamellar crystals, so it follows that the type of crystallinity is not a major factor, at least up to moderate strains. At higher strains, significantly lower stress levels in the blend compared to the corresponding copolymer suggested that the network structure and phase morphology may affect strain hardening.

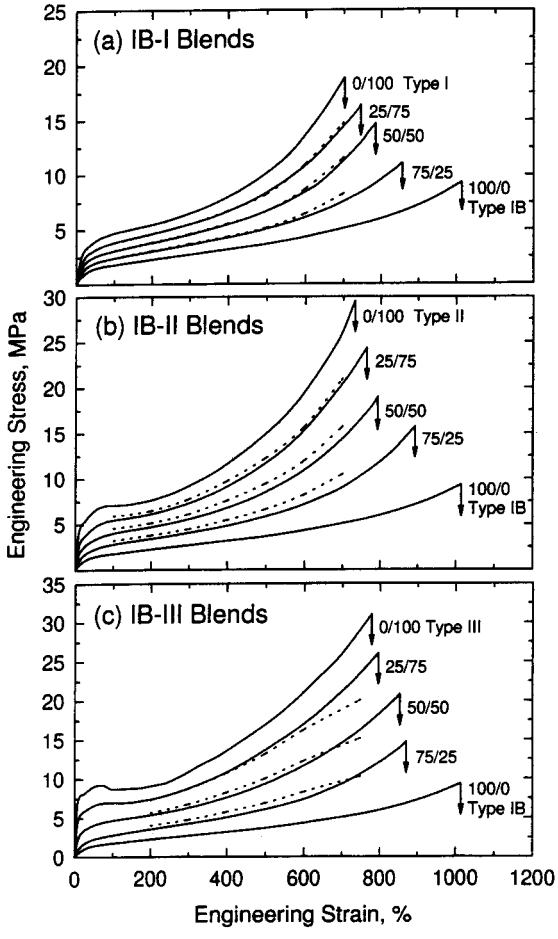

Figure 7 Stress–strain curves of blends: (a) Type IB-I blends; (b) Type IB-I blends; and (c) Type IB-III blends

In summary, the homogeneous comonomer composition and the large range in comonomer content of INSITE™ copolymers presented an opportunity to probe the effect of branch concentration on the solid state structure and properties of ethylene–octene copolymer blends. A low density copolymer (0.865 g cm^{-3}) was combined separately with three other copolymers of increasingly higher density (0.887, 0.901 and 0.913 g cm^{-3}). Results from classical techniques of polymer characterization, which are often ambiguous for blends of conventional, heterogeneous ethylene copolymers, were more revealing for INSITE™ copolymer blends. The components appeared to crystallize as two separate populations in all the blends, even in blends that combined two low density copolymers that were thought to form fringed micellar crystals. However, miscibility of the noncrystalline portions correlated with a previously proposed classification scheme based on density or comonomer content. Thus, blends of two Type I copolymers appeared to form a single noncrystalline phase, whereas the noncrystalline regions of blends that combined a Type I copolymer with a Type II or Type III copolymer appeared to be phase separated.

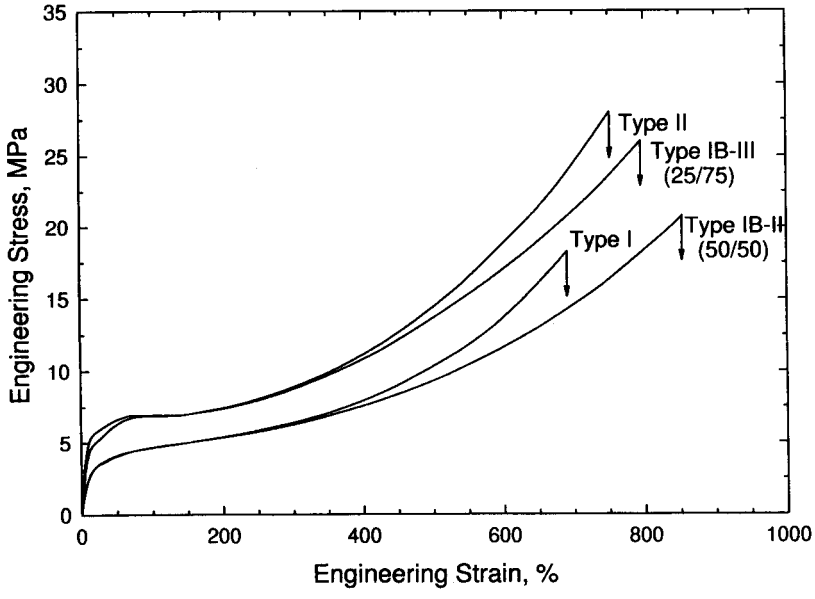

Figure 8 Two examples comparing the stress–strain curves of components and blends of the same density

ACKNOWLEDGEMENTS

The authors thank Mr Nadim Qureshi for his assistance with the mechanical measurements. The financial support of The Dow Chemical Company is gratefully acknowledged.

REFERENCES

1. Wilfong, D. L. and Knight, G. W., *J. Polym. Sci.: Part B: Polym. Phys.*, 1990, **28**, 861.
2. Hosoda, S., *Polym. J.*, 1988, **20**, 383.
3. Nesarikar, A., Crist, B. and Davidovich, A., *J. Polym. Sci.: Part B: Polym. Phys.*, 1994, **32**, 641.
4. Channell, A. D., Clutton, E. Q. and Capaccio, G., *Polymer*, 1994, **35**, 3893.
5. Mirabella, F. M., Westphal, S. P., Fernando, P. L., Ford, E. A. and Williams, J. G., *J. Polym. Sci., Polym. Phys. Edn.*, 1988, **26**, 1995.
6. Defoor, F., Groeninckx, G., Reynaers, H., Schouterden, P. and Van der Heijden, B., *J. Appl. Polym. Sci.*, 1993, **47**, 1839.
7. Hu, S.-R., Kyu, T. and Stein, R. S., *J. Polym. Sci.: Part B: Polym. Phys.*, 1987, **25**, 71.
8. Kyu, T., Hu, S.-R. and Stein, R. S., *J. Polym. Sci.: Part B: Polym. Phys.*, 1987, **25**, 89.
9. Datta, N. K. and Birley, A. W., *Plast. Rub. Proc. Appl.*, 1982, **2**, 237.
10. Abraham, D., George, K. E. and Francis, D. J., *Makromol. Chem.*, 1992, **200**, 15.
11. Minick, J., Moet, A. and Baer, E., *Polymer*, 1995, **36**, 1923.
12. Hill, M. J., Barham, P. J. and van Ruiten, J., *Polymer*, 1993, **34**, 2975.
13. Alamo, R. G., Glaser, R. H. and Mandelkern, L., *J. Polym. Sci.: Part B: Polym. Phys.*, 1988, **26**, 2169.
14. Graessley, W. W., Krishnamoorti, R., Balsara, N. P., Butera, R. J., Fetters, L. J., Lohse, D. J., Schulz, D. N. and Sissano, J. A., *Macromolecules*, 1994, **27**, 3896.
15. Crist, B. and Nesarikar, A. R., *Macromolecules*, 1995, **28**, 890.
16. Failla, M. D. and Mandelkern, L., *Macromolecules*, 1993, **26**, 7167.
17. Sehanobish, K., Patel, R. M., Croft, B. A., Chum, S. P. and Kao, C. I., *J. Appl. Polym. Sci.*, 1994, **51**, 887.
18. Minick, J., Moet, A., Hiltner, A., Baer, E. and Chum, S. P., *J. Appl. Polym. Sci.*, 1995, **58**, 1371.
19. Bensason, S., Minick, J., Moet, A., Chum, S., Hiltner, A. and Baer, E., *J. Polym. Sci.: Part B: Polym. Phys.*, 1996, **34**, 1301.
20. Mathot, V. B. F., in *Calorimetry and Thermal Analysis of Polymers*, ed. V. B. F. Mathot. Hanser, New York, 1994, Ch. 9.
21. Barham, P. J., Hill, M. J., Keller, A. and Rosney, C. C. A., *J. Mater. Sci. Lett.*, 1988, **7**, 1271.
22. Hill, M. J., Organ, S. J. and Barham, P. J., *Thermochim. Acta*, 1994, **238**, 17.
23. Alamo, R. G., Londono, J. D., Mandelkern, L., Stehling, F. C. and Wignall, G. D., *Macromolecules*, 1994, **27**, 411.